Biogeosciences Discuss., https://doi.org/10.5194/bg-2018-82
Manuscript under review for journal Biogeosciences
Discussion started: 27 February 2018

A refinement of coccolith separation methods: Measuring the sinking characters of coccoliths

Hongrui Zhang[1, 2], Heather Stoll[2], Clara Bolton[3], Xiaobo Jin[1], Chuanlian Liu[1]

[1] State Key Laboratory of Marine Geology, Tongji University, Shanghai, 200092, China

[2] Geological Institute, Department of Earth Science, Sonneggstrasse 5, ETH, 8092, Zürich, Switzerland

[3] Aix-Marseille Univ, CNRS, IRD, Coll de France, CEREGE, Aix en Provence, France.

Correspondence to: Chuanlian Liu (liucl@tongji.edu.cn)

Abstract. The sinking velocities of individual coccoliths are relevant for export of their CaCO3 from the surface ocean, and for laboratory methods to separate coccoliths of different sizes and species for geochemical analysis. In the laboratory, the repeat settling/decanting method was the earliest method to separate coccolith from sediments for geochemical analyses, and is still widely used. However, in the absence of estimates of settling velocity for non-spherical coccoliths, previous implementations have depended mainly on time consuming empirical method development by trial and error. In this study, the sinking velocities of coccoliths belonging to different species were carefully measured in a series of settling experiments for the first time. Settling velocities of modern coccoliths range from 0.154 to 10.67 cm h^{-1}. We found that a quadratic relationship between coccolith length and sinking velocity fits well and coccolith sinking velocity can be estimated by measuring the coccolith length and using the length-velocity factor, k_{sv}. We found a negligible difference in sinking velocities measured in different vessels. However, an appropriate choice of vessel must be made to avoid 'hindered settling' in coccolith separations. The experimental data and theoretical calculations presented here will support and improve the repeat settling/decanting method.

Biogeosciences Discuss., https://doi.org/10.5194/bg-2018-82
Manuscript under review for journal Biogeosciences
Discussion started: 27 February 2018

1. Introduction

Coccolithophores are some of the most important phytoplankton in the ocean. They can secrete calcareous plates called coccoliths, which contribute significantly to discrete particulate inorganic carbon in the euphotic zone and to $CaCO_3$ fluxes to the deep ocean (e.g., Young and Ziveri, 2000; Sprengel et al., 2002), and record paleoenvironmental changes (e.g., Beaufort et al., 1997; Stoll et al., 2002; Zhang et al., 2016). However, the use of coccolith geochemical analyses in paleoenvironmental reconstructions is hindered by the difficulty of isolating coccolith compared with foraminifera. Two main methods have been developed to concentrate near-monospecific assemblages of coccoliths from bulk sediments: one is the method based on a decanting technique (Paull and Thierstein, 1987; Stoll and Ziveri, 2002) and the other is that based on microfiltration (Minoletti et al., 2008). The improvement of separation techniques offered a new perspective to study the Earth's history (e.g. Stoll, 2005; Beltran et al., 2007; Bolton and Stoll, 2013; Rousselle et al., 2013; Tremblin et al, 2016). Moreover, the development of coccolith oxygen and carbon isotope studies in culture in recent years (e.g. Ziveri et al., 2003; Rickaby et al., 2010; Hermoso et al., 2016; McClelland et al., 2017) has provided an improved mechanistic understanding of coccolith isotope data and therefore stimulated the need for more purified coccolith fraction samples from the fossil record.

Both decanting and microfiltering are widely used methods for coccolith separation. Microfiltering relies heavily on the specifications of micro filter membrane (such as 2μm, 3μm, 5μm and 8μm pore size) and is highly effective in the large size range, but is very time consuming in sediments with a high proportion of very small coccoliths. It is also impossible to separate coccoliths with similar lengths by microfiltration, such as *Florisphaera profunda* and *Emiliania huxleyi* (Hermoso et al., 2015) Decanting, on the other hand, is highly effective for the small-sized coccoliths, because their slow settling times permit greater ability to separate different sizes. Consequently, in some studies, a combination of the micro filtering and sinking or centrifugation method were applied for coccolith separation (Stoll, 2005; Hermoso et al., 2015). The repeated sinking/decanting method, first employed by (Edwards, 1963; Paull and Thierstein, 1987) follows the simple principle formalized by Stokes' Law for spherical particles: particles of larger size settle more quickly because they have a higher ratio of volume and mass (accelerating sinking) to sectional

Biogeosciences Discuss., https://doi.org/10.5194/bg-2018-82
Manuscript under review for journal Biogeosciences
Discussion started: 27 February 2018

area (resistance retarding sinking). However, the sinking velocities of coccoliths with complex shape are difficult to calculate and have not been quantified in previous studies. Consequently, the repeated decanting method has generally used settling times based on empirical trial and error.

In this current study, we present a novel and rigorous estimation of the sinking velocity for 16 species of modern and Cenozoic coccoliths, carefully measured in 0.2% ammonia at 20℃. With this new dataset, we explore how to estimate the sinking velocity of coccoliths by shape and length, which allows our estimations to be generalized for other species, and for situations where the mean thickness of coccoliths of a given species was different from that of our study. These generalizations, together with our results on sinking velocities of one coccolith species (*Gephyrocapsa oceanica*) in different vessels, should allow a significant improvement in efficiency of future protocols for separation of coccoliths by repeated decanting.

2. Materials and methods

2.1 Sample selections

We measured the sinking velocity of 16 different species of coccoliths, principally of Quaternary age but including two Neogene samples (Figure 1). Numbers of small coccoliths, including *E. huxleyi*, *Gephyrocapsa* spp and *Reticulofenestra* spp. are about a magnitude greater than that of larger coccoliths. However, the larger coccoliths' contributions to carbonate can be as high as 50% (Baumann, 2004; Jin et al., 2016). Moreover, both small coccoliths and large coccoliths are useful in geochemical analyses (Ziveri et al., 2003; Rickaby et al., 2010; Candelier et al., 2013; Bolton et al., 2012, 2016; Bolton and Stoll, 2013). Therefore, both small and large coccoliths were studied in this research. The coccoliths were isolated from eight samples from the Pacific and Atlantic Oceans (more location information are in Figure 1 and Table A1; the pictures of studied coccolith can be found in Appendix B). All classifications of coccolith follow Nannotax3 except *Reticulofenestra* spp. (Figure C2 in Appendix C).

2.2 Experiment designs

2.2.1 Sample pretreatments

The sinking velocity measurement depends on absolute abundance estimation (more details in 2.2.2). However, on microscope slides, larger coccoliths and foraminifer fragments may cover smaller

Biogeosciences Discuss., https://doi.org/10.5194/bg-2018-82
Manuscript under review for journal Biogeosciences
Discussion started: 27 February 2018

coccoliths, reducing the accuracy of coccolith absolute number. Thus, before sinking experiments were carried out, raw sediments were pretreated to purify the target coccoliths to reduce errors in coccolith counting. The raw sediments were disaggregated in 0.2% ammonia and sieved through a 63 μm sieve and then treated by sinking method or filtering method (Bolton et al., 2012; Minoletti et al., 2008) to concentrate the target species up to at least more than 50% of total assemblages (for Noëlaerhabdaceae coccoliths, a percentage more than 90% can be easily achieved). Most of species were measured individually in settling experiments, except the *Pseudoemiliania lacunosa* and *Umbilicosphaera sibogae*, which cannot be separated from each other.

2.2.2 Measuring the sinking speeds of coccoliths

We are not aware of any prior direct determination of the sinking velocity of individual coccoliths, although the sinking velocities of live coccolithophores and other marine algae cells have been successfully measured by the 'FlowCAM' method (Bach et al., 2012) or similar photography technique (e.g. Miklasz and Denny, 2010). Here we introduce a simple method to measure the particle sinking speeds without special equipment. After pretreatment, the coccolith suspensions were gently shaken and then moved into comparison tubes which were vertically mounted on tube shelves. We set the timer going and let the suspension settle for a specified period of time, marked as sinking time or settling duration (T). Thereafter, we removed the upper 15 ml supernatant in a 50 ml centrifuge tube with a 10 ml pipette. This operation should be performed slowly and gently to avoid drawing lower suspensions upward. The number of coccoliths in the upper and lower suspensions were carefully counted by the 'drop technique', which is a quick method to determine absolute abundance of coccoliths (Koch and Young, 2007; Bordiga et al., 2015).

To calculate the sinking velocities of coccoliths, we define a parameter named the separation ratio (R), which represents the percentage of removed coccoliths in one separation. This parameter is important and will be repeatedly mentioned in the following part. R was measured using the following equation (more details about derivation can be found in Appendix D):

$$R = \frac{\frac{N1}{n1} \times V1}{\frac{N1}{n1} \times V1 + \frac{N2}{n2} \times V2} \quad (2\text{-}1)$$

where N1 and N2 are numbers of coccoliths counted in upper and lower suspension slides, respectively; n1 and n2 are the number of fields of view (FOV) counted. V1 and V2 are the volume of the settling vessel defined by the settling distance, as shown in Figure 2.

Biogeosciences Discuss., https://doi.org/10.5194/bg-2018-82
Manuscript under review for journal Biogeosciences
Discussion started: 27 February 2018

109 The separation ratio, R, also has a relationship with sinking time, T:

110 $$R = \frac{V_1 - \frac{V_1}{D} \times sv \times T}{V_1 + V_2} \quad (2\text{-}2)$$

111 where V1, V2 and D are shape parameters shown in Figure 2; and sv is the average sinking velocity
112 of measured coccoliths. If we plot R against T, the slope of line has a relationship with sv. Hence
113 liner regressions between R and T were processed with MATLAB to calculate the sv (details about
114 error analyses can be found in Appendix E).
115 There are still two issues to be explained. The first one is to eliminate the shape differences among
116 vessels, all separation ratios have been transferred to calibrated separation ratios (Rcal), which
117 means the separation ratio measured in a standard vessel (more details in Appendix D). The other
118 one is that we treated the average sinking velocities as the sinking velocities of the coccoliths with
119 the average length. This approximation has been proved reasonable in Appendix D.

120 **2.2.3 Detecting the potential influence of vessels**

121 Seven commonly used vessels were selected to detect the potential influence of vessels (Figure 3).
122 Two of them are made of plastics (No.2 and No.3 in Figure 3) and all others are pyrex glass vessels.
123 About 500 mg of sediment from the core KX21-2 were pretreated as described in 2.2.1 and
124 suspended in about 500 ml ammonia. After that, settling experiments were performed as described
125 in 2.2.2 using different vessels. In these experiments, only the dominant species, *G. oceanica*, was
126 measured.

127 **2.2.4 Other factors influencing the sinking velocity**

128 Temperature can change the density and viscosity of liquid. Generally speaking, the higher the
129 temperature is, the lower the density and viscosity will become and the faster pellets will sink. Take
130 water for instance, if the temperature increases from 15 to 30℃, the particle sinking velocity will
131 increase by ~43% (Table 1). All sinking velocities measured or discussed in the following sections
132 were velocities at 20℃ to minimize the influence of temperature.
133 The calibration of sinking velocity in high concentration suspension has been calculated by
134 Richardson and Zaki (1954)

135 $$sv = sv_0(1 - \alpha_s)^{2.7} \quad (2\text{-}3)$$

136 where the α_s is the solids volume fraction. Based on equation 2-3, the higher the suspension
137 concentration is, the slower the sinking velocity will be. That is so called 'hindered settling'. When

the α_s=0.2%, the reduction of sinking velocity owing to hindred settling cannot be neglectable (sv/sv_0 equals 99.46%). Hence, in this study all suspensions have solid volume fractions lower than 0.2% to avoid notable reduction of coccolith sinking velocities.

3. Results and Discussions

3.1 Influence of vessels

The sinking velocities of *G. oceanica* in the core KX21-2 in ammonia at 20℃ measured in different vessels vary from 0.99 to 1.23 cm h^{-1}. The lowest value occurred in the 100 ml centrifuge tube and the highest sinking velocity was measured in the 50 ml centrifuge tube experiments. The correlations between sinking velocities and different vessel parameters are quite low: r=0.13 for the vessel inner diameter, r=0.0005 for the sinking distance and r=0.051 for the upper volume and total volume ratio (V1/(V1+V2)). The dissipation of energy by friction between the moving fluid and the walls can cause a reduction of sinking speed (wall effect). A significant wall effect will be detected when a particle is settling in a vessel which diameter is smaller than the particle size by two orders of magnitude (Barnea and Mizarchi, 1973). The length of coccolith is on micron scales, so the diameters of vessel used in laboratory are about more than three order of magnitude larger than coccoliths. Moreover, our results show that the difference between vessel materials, glass and plastics, can also be ignored (Figure 4). Hence, we suggest that vessel type almost has no significant influence on sinking velocity of coccoliths.

However, our experiments were premised on the basis that the concentration of suspension was equal among different vessels. This means that large vessels can treat more sediment at one time but if we choose a larger vessel, more suspensions should be pumped and it often costs more time in sinking (often due to longer sinking distance). Assuming that the sediment is composed of 50% calcite (with density of 2.7 g cm^{-3}) and 50% clay (about 1.7 g cm^{-3}), the largest amount of sediment that can be used without significant reduction of the sinking velocity (5%) is about 400 mg in 100 ml suspension (this calculation is based on equation 2-3). However, the sediments accumulating in the lower suspension, the particle concentration can be more than 4 times higher than the initial homogenous concentration. To avoid this, we recommend about 100 mg dry sediment should be suspended in at least 100 ml suspension to avoid ‘hindered settling’. If more sediment is necessary

Biogeosciences Discuss., https://doi.org/10.5194/bg-2018-82
Manuscript under review for journal Biogeosciences
Discussion started: 27 February 2018

for geochemistry analyses, then a larger vessel should be selected to separate enough sample in one time.

3.2 Sinking velocities at 20℃ in 0.2% ammonia

We measured the separation ratios of different coccoliths in comparison tubes at 20℃ in 0.2% ammonia (Figure 5). The sinking velocities of coccoliths were then calculated by linear fitting of separation ratios and settling durations. The sinking velocities of studied coccoliths vary by one order of magnitude from 0.154 cm h^{-1} to 10.67 cm h^{-1} (Table 2). The highest sinking velocity was found in the measurement of *Coccolithus pelagicus* and the lowest velocity was found for *F. profunda*. The average sinking speeds of coccolith is about 10-50% of the terminal sinking velocities of calcite spheres calculated by Stokes' Law (Figure 6). These ratios are comparable with the oval objects (e.g. seeds) data from Xie and Zhang (2001) and smaller than those from McNown and Malaika (1950). The sinking velocities of coccoliths measured in our experiment are about 2-3 orders of magnitude smaller than values from sediment traps of 143-243 m d^{-1} (595~1012 cm h^{-1}) in the North Atlantic (Ziveri et al., 2000 and Stoll et al., 2007), confirming the fact that the coccoliths sinking out of the euphotic layer are mainly in the form of sinking aggregates rather than individual coccoliths.

3.3 Estimating the sinking velocities

Generally speaking, the sinking velocities of coccoliths increase with the distal shield length (Figure 5a), as expected from the increase in volume to sectional area for a given geometry as length increases. Our data implies that the sinking velocity has a power function relationship with distal shield length.

We propose that the sinking velocity of coccoliths might have a quadratic relationship with distal shield length as described by Stokes' Law (Figure 6a). If we use data for all species except *Helicosphaera carteri*, the sinking velocities can be described by the following equation:

$$sv = 0.0982\ (\pm 0.001) * \phi^2 \quad (3\text{-}1)$$

Based on this quadratic regression, we derive a shape-velocity factor (k_{sv}) that relates settling velocity to coccolith length.

$$sv = k_{sv} * \phi^2 \quad (3\text{-}2)$$

Biogeosciences Discuss., https://doi.org/10.5194/bg-2018-82
Manuscript under review for journal Biogeosciences
Discussion started: 27 February 2018

194 Furthermore, this factor is analogous to the shape-mass factor, 'k_s' used to relate coccolith mass to
195 coccolith length (Young and Ziveri, 2000). The length and shape-velocity factor of coccoliths can
196 be used to predict most of the sinking velocity variations, however, variations may also arise due to
197 changes in coccolith mass and thickness, for a given length, and due to the hydrodynamics of
198 particular shapes. We noticed that the smaller coccolith *G. caribbeanica* has a greater sinking
199 velocity than the larger coccolith, *G. oceanica*. We suggest that this was caused by greater mass per
200 length (or greater average thickness) in the case of *G. caribbeanica* and this may be due to the closed
201 central area while *G. oceanica* has an open central area. Another example is H. carteri, its smaller
202 sinking velocity can be explained by the unique structure: the broad edge of *H. carteri* can increase
203 the drag force significantly and *H. carteri* has the largest ellipticity (major axis length and minor
204 axis length ratio) among the measured coccoliths, which means the mass of *H. carteri* is smaller
205 than other species of coccoliths with similar lengths (Figure 6d and Figure C3). In the case of partial
206 dissolution, the well-preserved *Cyclicargolithu floridanus* may have higher mass than dissolved (or
207 disarticulated) *Cy. floridanus*, and therefore a slightly higher shape-velocity factor.

208 **4. Conclusions**

209 To improve coccolith separation by settling methods, we measured sinking velocities of different
210 coccoliths by gravity. Sinking velocities in this study varied from 0.154 to 10.61 cm h^{-1}, about 10%
211 to 50% of those of calcite spheres with same diameter. The shape of different vessels had little
212 impact on the sinking velocity. But we should consider the volume of vessels to avoid 'hindered
213 settling'. The sinking velocities are mainly controlled by the shape of coccolith, including the distal
214 shield length, the size of central area, and the ellipticity of coccoliths. Besides the shape of coccoliths,
215 temperature is also crucial to the coccolith separations because of the dependence of sinking
216 velocities on temperature.

217 Length-velocity factors were proposed to estimate coccoliths sinking velocities, so coccolith sinking
218 speeds in different samples can be easily estimated by following steps:

219 **1.** Measure the mean length of coccoliths under the microscope;

220 **2a.** For species which sinking speed has been directly measured, we can use the length-velocity
221 factor directly ($sv=k_{sv}* \phi^2$);

222 **2b.** For unmeasured species, we can choose the length-velocity factor of coccolith with similar

morphology in this study or use the general length-velocity formula (sv=0.098(±0.001)* ϕ^2) If we use the general formula, it should be noted that a closed central area coccolith will sink faster than prediction (for *G. caribbeanica* and small *C. leptoporus* will settle ~40% faster) and coccoliths with greater ellipticity can settle much slower (for *H. carteri* will settle as 30% of the predicted sinking velocity for coccolith with similar length).

Acknowledgements. This study was supported by grants from the Chinese National Science Foundation (91428310, 91428309 and 41530964, to L.C.). We thank the Integrated Ocean Drilling Program (IODP) for providing the samples. The IODP is sponsored by the U.S. National Science Foundation and participating countries under management of the IODP Management International, Inc (IODP-MI).

Biogeosciences Discuss., https://doi.org/10.5194/bg-2018-82
Manuscript under review for journal Biogeosciences
Discussion started: 27 February 2018

234 **Table 1.** The influence of temperature on sinking velocity. Density data is from Kell (1975) and
235 viscosity data is from Joseph et al. (1978).

T (℃)	ρ (g cm^{-3})	η (mPa s)	$SV_T : SV_{T=20}$
15	0.9991	1.1447	0.8804
20	0.9982	1.0087	1
25	0.9970	0.8949	1.1279
30	0.9956	0.8000	1.2627

236 **Table 2.** The sinking velocity and shape-velocity factor of different coccolith species: ϕ means the
237 distal shield length of coccolith and St ϕ is the standard deviation of distal shield length; sv represents
238 the sinking velocity; sv (95%-) and sv (95%+) represent the lower and higher limit of 95% confidence
239 level, respectively. 'k_{sv}' represents the length-sinking velocity factor. The short name of coccolith can
240 be found in the caption of Figure 4. The details of coccoliths length distribution are in Appendix C.

Species	abb.	ϕ (μm)	St ϕ (μm)	sinking velocity (cm h^{-1})	Sv (95% -)	Sv (95% +)	k_{sv}
F. profunda	Fp-WP	1.508	0.557	0.158	0.010	0.011	0.070
F. profunda	Fp-SCS	1.786	0.641	0.154	0.051	0.052	0.048
small *Reticulofenestra*	Ret (<4um)	2.454	0.509	0.848	0.354	0.416	0.141
E. huxleyi	Emi	2.512	0.469	0.853	0.054	0.064	0.135
Gephyocapsa spp.	G spp	2.755	0.502	0.752	0.125	0.147	0.099
G. caribbeanica	Gcar	3.312	0.352	1.873	0.174	0.192	0.171
U. sibogae	Umb	4.060	0.500	1.268	0.416	0.441	0.077
G. oceanica	Geo	4.187	0.517	1.170	0.155	0.178	0.067
P. lacunosa	Pla	4.350	0.617	1.171	0.337	0.338	0.062
Small *Ca. leptoporus*	Cal small	4.605	0.629	3.351	0.172	0.199	0.158
large *Reticulofenestra*	Ret(>4um)	4.988	0.605	2.379	0.534	0.641	0.096
Cy. floridanus	Cyf	5.805	0.963	4.174	0.320	0.336	0.124
(dissolved) *Cy. floridanus*	Cyf -d	6.134	0.727	4.508	0.352	0.417	0.120
Large *Ca. leptoporus*	Cal large	6.370	0.931	3.737	1.053	1.336	0.092
H. carteri	Hel	8.936	0.994	2.541	1.740	2.440	0.032
Co. pelagicus	Cpl	10.640	1.175	10.610	0.950	1.235	0.094

241

Biogeosciences Discuss., https://doi.org/10.5194/bg-2018-82
Manuscript under review for journal Biogeosciences
Discussion started: 27 February 2018

242 **Figure 1**. Temporal and spatial distribution of samples. (a) The evolution of studied coccoliths: first
243 occurrence and last occurrence data are from Nannotax3
244 (http://www.mikrotax.org/Nannotax3/index.html). The blue bars represent ranges of first occurrence
245 and the green bars represent ranges of last occurrence. The blue diamonds represent samples used in
246 this study. (b) Spatial distribution of samples. 1304 means IODP U1304, 3428 means MD12-3428cq,
247 1433 and 1435 means IODP U1433 and U1435, respectively. 807 means ODP 807 and 21-2 means
248 KX21-2.

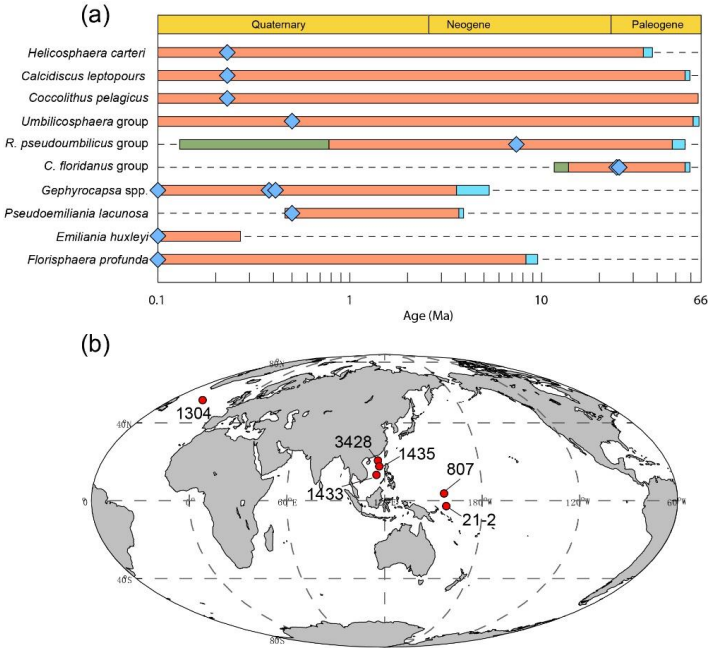

249

Biogeosciences Discuss., https://doi.org/10.5194/bg-2018-82
Manuscript under review for journal Biogeosciences
Discussion started: 27 February 2018

250

251 **Figure 2.** Schematic of settling experiments. The pictures were taken after *Coccolithus pelagicus*
252 sinking experiments with T=0 and T=30 min. V1 and V2 are the volumes of the upper and lower
253 cylinders, D is the settled distance.

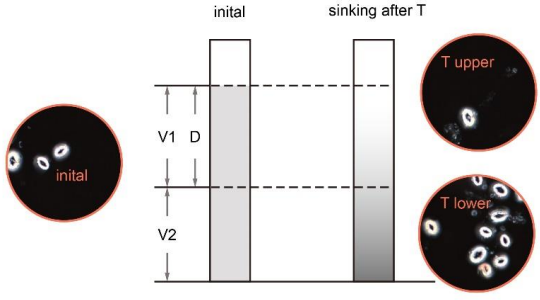

254

Biogeosciences Discuss., https://doi.org/10.5194/bg-2018-82
Manuscript under review for journal Biogeosciences
Discussion started: 27 February 2018

Figure 3. The shape parameters of vessels. V1 and V2 means the volume of upper suspension and lower suspension, respectively. D means sinking distance. Φ means average inner diameter which is calculated by $V1/(\pi D^2)$.

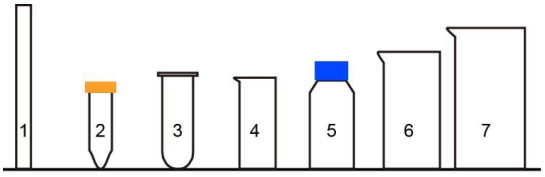

No.	Name	V1	V2	D (cm)	Φ (cm)
1	25 ml comparsion tube	15	10	6.376	1.73
2	50 ml centrifuge tube	30	20	5.480	2.64
3	100 ml centrifuge tube	50	30	4.854	3.62
4	100 ml beaker	40	40	2.834	4.24
5	100 ml reagent bottle	40	40	1.900	5.18
6	250 ml beaker	150	100	4.400	6.59
7	500 ml beaker	300	200	5.700	8.19

Biogeosciences Discuss., https://doi.org/10.5194/bg-2018-82
Manuscript under review for journal Biogeosciences
Discussion started: 27 February 2018

260 **Figure 4.** Sinking velocities of *G. oceanica* in the core KX-21-2 measured in different vessels. (a) The
261 calibrated separation ratios measured in different vessels. Error bars show 95% confidence level of
262 calibrated separation ratio. (b-d) The relationship between sinking velocity and different vessel shape
263 parameters. Error bars represent 95% confidence level of sinking velocity in each vessel and the shade
264 area represents 95% confidence level of sinking velocity considering all data points.

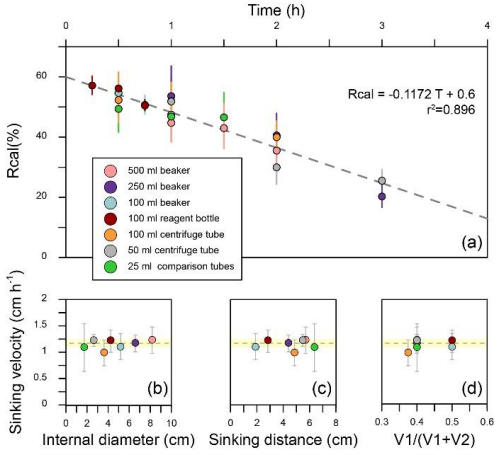

265

Biogeosciences Discuss., https://doi.org/10.5194/bg-2018-82
Manuscript under review for journal Biogeosciences
Discussion started: 27 February 2018

266 **Figure 5.** The calculated separation ratio (Rcal) vs sinking duration. Fp-WP means *F. profunda* in the
267 West Pacific. Fp-SCS means *F. profunda* in the South China Sea. Emi means *E. huxleyi*. Gspp means
268 small *Geophyocapsa*. Geo means *G. oceanica*. Gcarb means *G. caribbeanica*. Ret<4 means small
269 *Reticulofenestra*. Ret>4 means large *Reticuloenestra*. Cyf means *Cyclicargolithus floridanus*. Cy-d
270 means dissolved *Cy. floridanus*. Umb means *U. sibogae*. Pla means *Pseudomiliania lacunose*. Hel
271 means *Helicosphaera carteri*. Cal large means larger *Calicidiscus leptoporus*. Cal small means small
272 *Ca. leptoporus*. Cpl means *Co. pelagicus*.

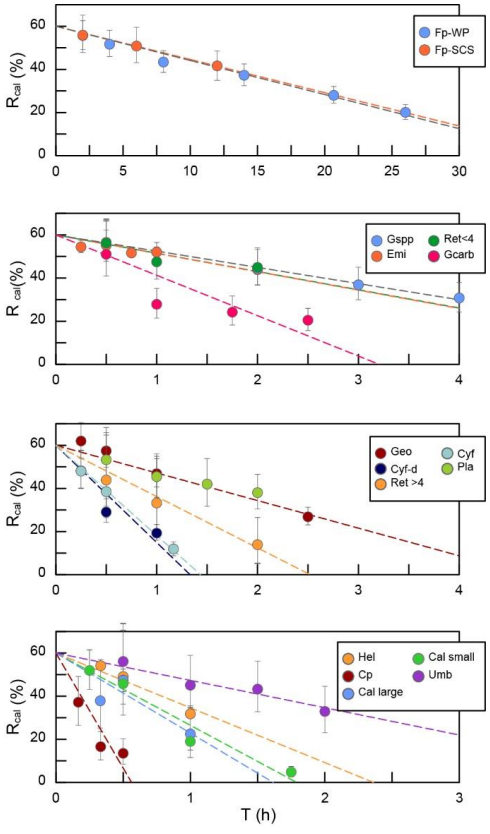

273
274

Biogeosciences Discuss., https://doi.org/10.5194/bg-2018-82
Manuscript under review for journal Biogeosciences
Discussion started: 27 February 2018

275

276 **Figure 6.** Coccolith sinking velocities and coccolith shape factors. (a-b) Sinking velocities and mean
277 distal shield length. The horizontal error bars represent one standard deviation of coccolith length and
278 the vertical ones represent 95% confidence level of measured sinking velocities. The blue, green and
279 red lines represent sinking velocity of calcite sphere objects, coccolith sinking velocities estimated by
280 Bolton et al. (2012) and this study, respectively. (c) The ratio of measured speed and speed calculated
281 by Stokes' Law. (d) Coccolith short axis length (SAL) and long axis length (LAL) ratio against shape-
282 velocity factor k_{sv}. Box shows median value and upper/lower quartiles, whiskers show maximum and
283 minimum values, outliers larger than 1.5 of the interquartile range are shown as red crosses. The SAL
284 against LAL plot was shown in Figure C3. The short names of coccoliths can be found in Table 2.

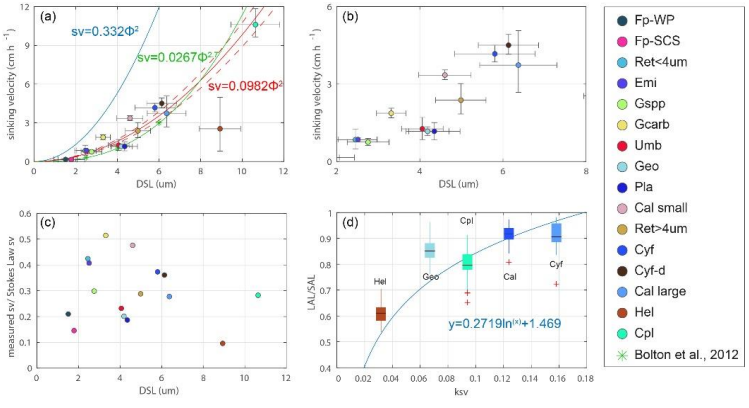

285

References

Bach, L.T., Riebesell, U., Sett, S., Febiri, S., Rzepka, P., Schulz, K.G., 2012. An approach for particle sinking velocity measurements in the 3-400 mum size range and considerations on the effect of temperature on sinking rates. Mar Biol 159, 1853-1864, doi:10.1007/s00227-012-1945-2.

Barnea, E., Mizrahi, J., 1973. A generalized approach to the fluid dynamics of particulate systems: Part 1. General correlation for fluidization and sedimentation in solid multiparticle systems. The Chemical Engineering Journal 5, 171-189, doi:10.1016/0300-9467(73)80008-5.

Baumann, K.-H., 2004. Importance of size measurements for coccolith carbonate flux estimates. Micropaleontology, 35-43.

Beaufort, L., Lancelot, Y., Camberlin, P., Cayre, O., Vincent, E., Bassinot, F., Labeyrie, L., 1997. Insolation cycles as a major control of equatorial Indian Ocean primary production. Science 278, 1451-1454, doi:10.1126/science.278.5342.1451.

Beltran, C., de Rafélis, M., Minoletti, F., Renard, M., Sicre, M.A., Ezat, U., 2007. Coccolith $\delta^{18}O$ and alkenone records in middle Pliocene orbitally controlled deposits: High-frequency temperature and salinity variations of sea surface water. Geochemistry, Geophysics, Geosystems 8, Q05003, doi:10.1029/2006GC001483.

Bolton, C.T., Hernandez-Sanchez, M.T., Fuertes, M.A., Gonzalez-Lemos, S., Abrevaya, L., Mendez-Vicente, A., Flores, J.A., Probert, I., Giosan, L., Johnson, J., Stoll, H.M., 2016. Decrease in coccolithophore calcification and CO2 since the middle Miocene. Nat Commun 7, 10284, doi:10.1038/ncomms10284.

Bolton, C.T., Stoll, H.M., 2013. Late Miocene threshold response of marine algae to carbon dioxide limitation. Nature 500, 558-562, doi:10.1038/nature12448.

Bolton, C.T., Stoll, H.M., Mendez-Vicente, A., 2012. Vital effects in coccolith calcite: Cenozoic climate-pCO2drove the diversity of carbon acquisition strategies in coccolithophores, Paleoceanography 27, doi:10.1029/2012pa002339.

Bordiga, M., Bartol, M., Henderiks, J., 2015. Absolute nannofossil abundance estimates: Quantifying the pros and cons of different techniques. Revue de micropaléontologie 58,

155-165 doi:10.1016/j.revmic.2015.05.002.

Candelier, Y., Minoletti, F., Probert, I., Hermoso, M., 2013. Temperature dependence of oxygen isotope fractionation in coccolith calcite: A culture and core top calibration of the genus Calcidiscus. Geochimica et Cosmochimica Acta 100, 264-281, doi:10.1016/j.gca.2012.09.040.

Hermoso, M., Candelier, Y., Browning, T.J., Minoletti, F., 2015. Environmental control of the isotopic composition of subfossil coccolith calcite: Are laboratory culture data transferable to the natural environment? GeoResJ 7, 35-42, doi:10.1016/j.grj.2015.05.002.

Hermoso, M., Chan, I.Z.X., McClelland, H.L.O., Heureux, A.M.C., Rickaby, R.E.M., 2016. Vanishing coccolith vital effects with alleviated carbon limitation. Biogeosciences 13, 301-312, doi:10.5194/bg-13-301-2016.

Jin, X., Liu, C., Poulton, A.J., Dai, M., Guo, X., 2016. Coccolithophore responses to environmental variability in the South China Sea: species composition and calcite content. Biogeosciences 13, 4843-4861, doi: 10.5194/bg-13-4843-2016.

Kell, G.S., 1975. Density, thermal expansivity, and compressibility of liquid water from 0. deg. to 150. deg.. correlations and tables for atmospheric pressure and saturation reviewed and expressed on 1968 temperature scale. Journal of Chemical and Engineering Data 20, 97-105.

Kestin, J., Sokolov, M., Wakeham, W.A., 1978. Viscosity of liquid water in the range −8 °C to 150 °C. Journal of Physical and Chemical Reference Data 7, 941-948.

Koch, C., Young, J., 2007. A simple weighing and dilution technique for determining absolute abundances of coccoliths from sediment samples. J. Nannoplankton Res.

McClelland, H.L., Bruggeman, J., Hermoso, M., Rickaby, R.E., 2017. The origin of carbon isotope vital effects in coccolith calcite. Nat Commun 8, 14511, doi:10.1038/ncomms14511.

McClelland, H.L., Barbarin, N., Beaufort, L., Hermoso, M., Ferretti, P., Greaves, M., Rickaby, R.E.M., 2016. Calcification response of a key phytoplankton family to millennial-scale environmental change. Scientific Reports 6, 34263, doi: 10.1038/srep34263.

McNown, John S., and Jamil Malaika. "Effects of particle shape on settling velocity at low

Reynolds numbers." Eos, Transactions American Geophysical Union 31.1 (1950): 74-82.

Miklasz, K.A., Denny, M.W., 2010. Diatom sinkings speeds: Improved predictions and insight from a modified Stokes' law. Limnology and Oceanography 55, 2513-2525, doi:10.4319/lo.2010.55.6.2513.

Minoletti, F., Hermoso, M., Gressier, V., 2008. Separation of sedimentary micron-sized particles for palaeoceanography and calcareous nannoplankton biogeochemistry. Nat. Protocols 4, 14-24, doi:10.1038/nprot.2008.200.

Paull, C.K., Thierstein, H.R., 1987. Stable isotopic fractionation among particles in Quaternary coccolith-sized deep-sea sediments. Paleoceanography 2, 423-429, doi:10.1029/PA002i004p00423.

Edwards, A.R., 1963. A preparation technique for calcareous nannoplankton. Micropaleontology 9, 103-104.

Richardson, J., Zaki, W., 1954. The sedimentation of a suspension of uniform spheres under conditions of viscous flow. Chemical Engineering Science 3, 65-73.

Rickaby, R.E.M., Henderiks, J., Young, J.N., 2010. Perturbing phytoplankton: response and isotopic fractionation with changing carbonate chemistry in two coccolithophore species. Clim. Past 6, 771-785, doi:10.5194/cp-6-771-2010.

Rousselle, G., Beltran, C., Sicre, M.-A., Raffi, I., De Rafélis, M., 2013. Changes in sea-surface conditions in the Equatorial Pacific during the middle Miocene–Pliocene as inferred from coccolith geochemistry. Earth and Planetary Science Letters 361, 412-421, doi:10.1016/j.epsl.2012.11.003.

Sprengel, C., Baumann, K.-H., Henderiks, J., Henrich, R., Neuer, S., 2002. Modern coccolithophore and carbonate sedimentation along a productivity gradient in the Canary Islands region: seasonal export production and surface accumulation rates. Deep Sea Research Part II: Topical Studies in Oceanography 49, 3577-3598 doi: 10.1016/S0967-0645(02)00099-1.

Stoll, H.M., 2005. Limited range of interspecific vital effects in coccolith stable isotopic records during the Paleocene-Eocene thermal maximum. Paleoceanography 20, doi:10.1029/2004pa001046.

373 Stoll, H.M., Rosenthal, Y., Falkowski, P., 2002. Climate proxies from Sr/Ca of coccolith calcite:
374 calibrations from continuous culture of Emiliania huxleyi. Geochimica et Cosmochimica
375 Acta 66, 927-936, doi:10.1016/S0016-7037(01)00836-5.
376 Stoll, H.M., Ziveri, P., 2002. Separation of monospecific and restricted coccolith assemblages
377 from sediments using differential settling velocity. Marine Micropaleontology 46, 209-
378 221, doi: 10.1016/S0377-8398(02)00040-3.
379 Tremblin, M., Hermoso, M., Minoletti, F., 2016. Equatorial heat accumulation as a long-term
380 trigger of permanent Antarctic ice sheets during the Cenozoic. Proceedings of the National
381 Academy of Sciences 113, 11782-11787 doi: 10.1073/pnas.1608100113.
382 Xie, H-Y., and D-W. Zhang. "Stokes shape factor and its application in the measurement of
383 spherity of non-spherical particles." Powder Technology 114.1 (2001): 102-105 doi:
384 10.1016/S0032-5910(00)00269-2.
385 Young, J.R., Ziveri, P., 2000. Calculation of coccolith volume and it use in calibration of
386 carbonate flux estimates. Deep sea research Part II: Topical studies in oceanography 47,
387 1679-1700, doi:10.1016/S0967-0645(00)00003-5.
388 Zhang, H., Liu, C., Jin, X., Shi, J., Zhao, S., Jian, Z., 2016. Dynamics of primary productivity
389 in the northern South China Sea over the past 24,000 years. Geochemistry, Geophysics,
390 Geosystems 17, 4878-4891, doi:10.1002/2016GC006602 .
391 Ziveri, P., Stoll, H., Probert, I., Klaas, C., Geisen, M., Ganssen, G., Young, J., 2003. Stable
392 isotope 'vital effects' in coccolith calcite. Earth and Planetary Science Letters 210, 137-
393 149, doi:10.1016/S0012-821X(03)00101-8.

Biogeosciences Discuss., https://doi.org/10.5194/bg-2018-82
Manuscript under review for journal Biogeosciences
Discussion started: 27 February 2018

Appendix A. Sample selections

Table A1. Sample selections

Measured coccolith	abb.	Region	Core	Section	Epoch	Age model ref.
F. profunda	Fp-SCS	SCS	MD12-3428	0-1 cm	Holocene	Zhang et al., 2016
F. profunda	Fp-WP	W.P.	KX21-2	2-4 cm	Holocene	Liang et al., 2016
E. huxleyi	Emi	SCS	MD12-3428	0-1 cm	Holocene	Zhang et al., 2016
Gephyocapsa spp.	Gspp	W.P.	ODP 807A	1H 5W 102-104	Pleistocene	Jin et al., 2010
G. oceanica	Geo	W.P.	KX21-2	2-4 cm	Holocene	Liang et al., 2016
G. caribbeanica	Gcarb	N.A.	IODP 1304B	7H 5W 69-70	Pleistocene	Channell et al., 2010
small *Reticulofenestra*	Ret<4	SCS	IODP 1433B	28R 2W 30-34	Miocene	Li et al., 2013
large *Reticulofenestra*	Ret>4	SCS	IODP 1433B	28R 2W 30-34	Miocene	Li et al., 2013
Cyclicargolithus floridanus	Cyf	SCS	IODP 1435A	6R 3W 25-29	Oligocene	Li et al., 2013
Cyclicargolithus floridanus	Cyf-d	SCS	IODP 1435A	8R 1W 27-31	Oligocene	Li et al., 2013
Umbilicosphaera sibogae	Umb	W.P.	ODP 807A	3H 5W 92-94	Pleistocene	Jin et al., 2010
Pseudoemiliania lacunosa	Pla	W.P.	ODP 807A	3H 5W 92-94	Pleistocene	Jin et al., 2010
Helicosphaera carteri	Hel	W.P.	ODP 807A	3H 5W 92-94	Pleistocene	Jin et al., 2010
large *Calcidiscus leptoporus*	Cal large	W.P.	ODP 807A	3H 5W 92-94	Pleistocene	Jin et al., 2010
small *Calcidiscus leptoporus*	Cal small	N.A.	IODP 1304B	7H 5W 69-70	Pleistocene	Channell et al., 2010
Coccolithus pelagicus	Cpl	N.A.	IODP 1304B	7H 5W 69-70	Pleistocene	Channell et al., 2010

References:

Channell, J., Sato, T., Kanamatsu, T., Stein, R., Alvarez Zarikian, C., 2010. Expedition 303/306 synthesis: North Atlantic climate. Channell, JET, Kanamatsu, T., Sato, T., Stein, R., Alvarez Zarikian, CA, Malone, MJ, and the Expedition 303, 306.

Jin, H., Jian, Z., Cheng, X., Guo, J., 2011. Early Pleistocene formation of the asymmetric east-west pattern of upper water structure in the equatorial Pacific Ocean. Chinese Science Bulletin 56, 2251-2257.

404 Li, C.-F., Lin, J., Kulhanek, D.K., 2013. South China Sea tectonics: Opening of the South
405 China Sea and its implications for southeastAsian tectonics, climates, and deep mantle
406 processes since the late Mesozoic. IODP Sci. Prosp 349.
407 Liang, D., Liu, C., 2016. Variations and controlling factors of the coccolith weight in the
408 Western Pacific Warm Pool over the last 200 ka. Journal of Ocean University of China
409 15, 456-464.
410 Zhang, H., Liu, C., Jin, X., Shi, J., Zhao, S., Jian, Z., 2016. Dynamics of primary productivity
411 in the northern South China Sea over the past 24,000 years. Geochemistry, Geophysics,
412 Geosystems 17, 4878-4891.

Biogeosciences Discuss., https://doi.org/10.5194/bg-2018-82
Manuscript under review for journal Biogeosciences
Discussion started: 27 February 2018

413 **Appendix B. Coccolith images under circular polarized light**

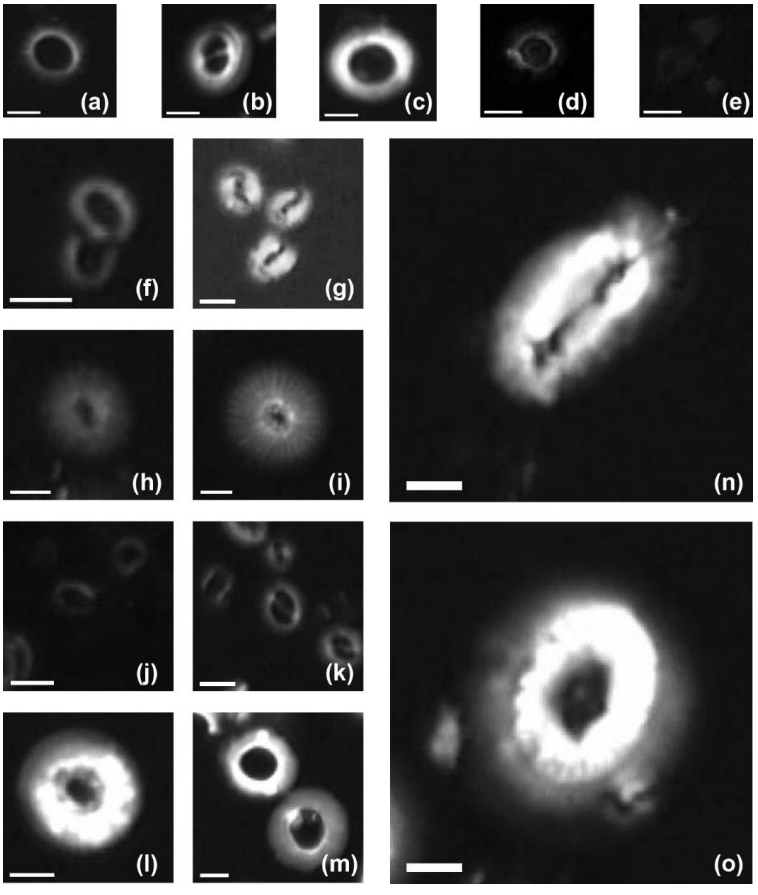

414

415 **Plate B1**. Imaged of measured coccolith in this study: (a) *Pseudoemiliania lacinosa* in the core ODP
416 807; (b) *Gephyrocapsa* oceanica in the core KX21-2; (c) *Reticulofenestra* spp. (large) in the core
417 IODP U1433B; (d) *Umbilicosphaera sibogae* in the core ODP 807; (e) *Florispharea profunda* in
418 the core KX21-2; (f) *Reticulofenestra* spp. (small) in the core IODP U1433B; (g) *Gephyrocapsa*
419 *caribbeanica* in the core IODP U1304B; (h) small *Calcidiscus leptopours* in the core IODP U1304B;
420 (i) large *Calcidiscus leptopours* in the core ODP 807A; (j) *Emiliania huxleyi* in the surface sediment
421 in the South China Sea; (k) *Gephyrocapsa* spp. in the core ODP 807; (l) *Cyclicargolithus floridanus*
422 in the core IODP U1435A and (m) dissolved *Cyclicargolithus floridanus* in the same core; (n)
423 *Helicosphaera carteri* in the core ODP 807A; (o) *Coccolithus pelagicus* in the core IODP U1304B.
424 White bars represent a length of 2 μm.

Biogeosciences Discuss., https://doi.org/10.5194/bg-2018-82
Manuscript under review for journal Biogeosciences
Discussion started: 27 February 2018

Appendix C. The length distribution of coccoliths

To measure the distal shield length of coccoliths, pictures were taken at a magnification of 1250x under circular polarized light. The coccolith lengths were measured by using the image analysis software, ImageJ. More than 5 pictures were taken and more than 50 (usually more than 100) coccolith specimens were measured. The length distributions of coccoliths measured in our experiments were shown in the Figure C1.

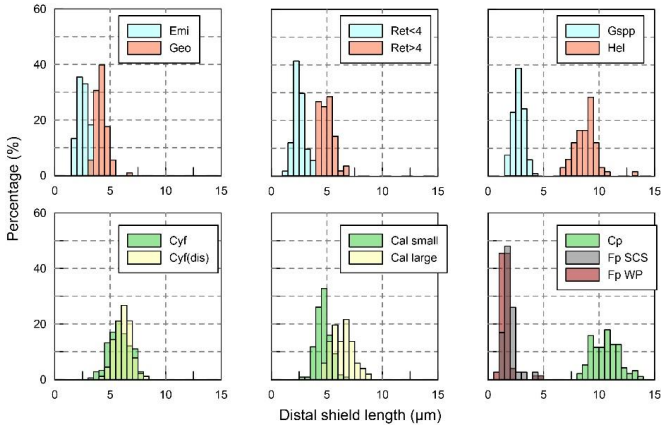

Figure C1. Size distribution of coccolith measured in the present study. The shorten names of coccolith follow Table A1.

The classification of coccoliths by length was supported by mixture analysis in PAST (Hammer et al., 2001), such as *Reticulofenestra* spp. and *Gephyrocapsa* spp. *Reticulofenestra* spp. in the Miocene were classified into two groups, Ret. (<4 μm) and Ret. (>4 μm). The traditional classification of *Reticulofenestra* spp. is <3 μm, 3-5 μm and 5-7 μm didn't pass the normal distribution test. Hence, in this study the *Reticulofenestra* spp. are divided at 4 μm (Figure C2). *Gephyrocapsa* spp. were classified by the shape of coccoliths into small *Gephyrocapsa* (central area opening and length <3.5 μm), *G. oceanica* (central area opening and length >3.5μm) and *G. caribbeanica* (closed central area) by the length and central area.

Biogeosciences Discuss., https://doi.org/10.5194/bg-2018-82
Manuscript under review for journal Biogeosciences
Discussion started: 27 February 2018

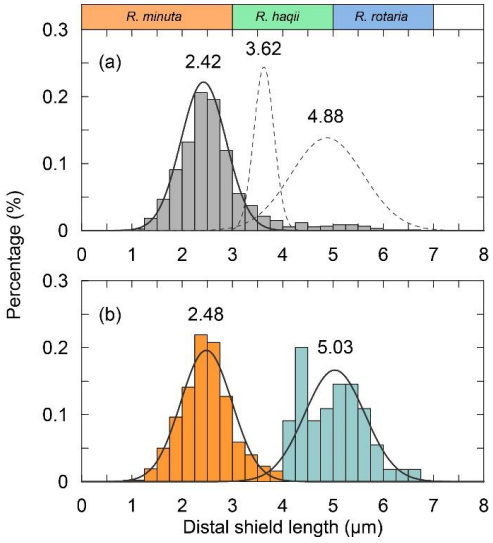

442

443 **Figure C2**. The classical classification of *Reticulofenestra* spp. (a) and the classification used in our

444 study (b). The curves represent the normal distribution fits of different coccolith groups and the dish

445 curve marks that the goodness of fit is below 0.2.

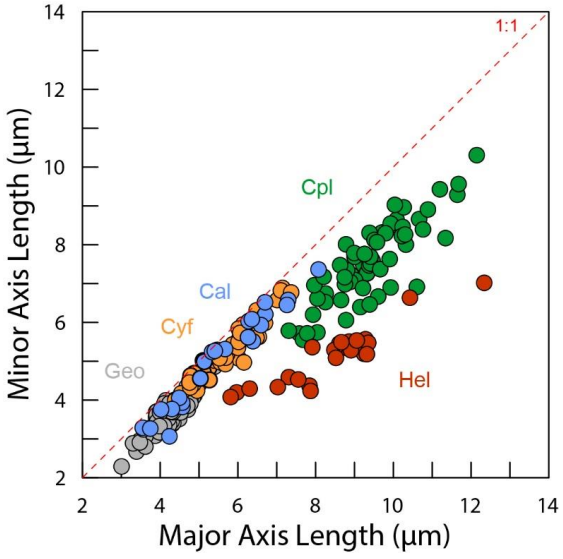

446

447 **Figure C3.** The short axis and long axis length distribution of coccoliths in Figure 6d.

448 **Reference.**

449 Hammer, Ø., Harper, D., Ryan, P., 2001. Paleontological Statistics Software: Package for
450 Education and Data Analysis. Palaeontologia Electronica.

Biogeosciences Discuss., https://doi.org/10.5194/bg-2018-82
Manuscript under review for journal Biogeosciences
Discussion started: 27 February 2018

Appendix D. Coccolith movement in gravity settling

In this part, the derivation of equation will be explained in detail including proofs of several assumptions mentioned in the methods part.

When the well mixed sediment begins to sink, the decrease of coccoliths number in the upper suspension (N_u) can be described as following equation:

$$\frac{dN_u}{dT} = -\frac{N_{u(t=0)}}{D} \times sv \quad \text{(D-1)}$$

where the D is the length of upper suspension and $N_{u(t=0)}$ /D is the initial number of coccolith in cross-section with a thickness of dD.

Do integration for the equation D-1, we can get the variation of coccolith number in the upper column over time:

$$N_u = N_{u(t=0)} - \frac{N_{u(t=0)}}{D} \times sv \times T \quad \text{(D-2)}$$

After a period of time (T), we pump out the upper suspension. Here we define the number of coccoliths in the upper supernatant dividing the total coccoliths number in the tube (Nt) as separation ratio (R), which represents the percentage of total coccoliths removed in one separation. This parameter is important and will be repeatedly mentioned in the following part. R can be expressed by

$$R = \frac{Nu}{Nt} \quad \text{(D-3)}$$

Assuming all coccoliths are uniformly distributed in the suspension at the beginning of settling, Nu(t=0) has relationship with Nt as follow:

$$\frac{Nu(t=0)}{Nt} = \frac{V1}{V1+V2} \quad \text{(D-4)}$$

where V1 is the volume of upper suspensions and V2 is the volume of lower suspensions.

Combining the equation D-1, D-2, D-3 and D-4, we obtain the relationship between separation ratio, R, and sinking velocity, sv, as follow:

$$R = \frac{N_u}{N_t} = \frac{N_{u(t=0)} - \frac{N_{u(t=0)}}{D} \times sv \times T}{N_t} = \frac{V_1 - \frac{V_1}{D} \times sv \times T}{V_1+V_2} \quad \text{(D-5)}$$

If we plot the R and T on a figure, the slope of the line is a function of V1, V2, D and sv. Since the V1, V2, D are known parameters, we say the slope of R-T is a function of sv, which is exactly what we want.

Biogeosciences Discuss., https://doi.org/10.5194/bg-2018-82
Manuscript under review for journal Biogeosciences
Discussion started: 27 February 2018

Comparison tubes used in our experiments have the same V1 and V2 but different D. Other vessels used in other experiments have different V1, V2 and D. So we should adjust the raw separation ratio to calibrated separation ratio (Rcal), which represents the separation ratio made in a standard vessel with V1=15 ml, V2=10 ml and D=6 cm. This step can be described by equation 2-6:

$$Rcal = \frac{[R\times(V1+V2)-V1]\times D\times 15}{(6\times V1+15)\times 25} \quad \text{(D-6)}$$

After calibrated, the slope of Rcal-T (k) has relationship with sv as following equation:

$$sv = -10 \times k \quad \text{(D-7)}$$

Hence, the sinking velocity of different coccolith can be achieved by measuring the variations of Rcal over time.

We also offer a test for the assumption that the average sinking velocity of all coccoliths can be treated as the sinking velocity of coccoliths with the average length. Here we used the data of G. oceanica. A normal distribution was fitted to the measured length distribution (Figure D1-a). And then we simulate a normal distribution situation of coccoliths in the vessel. The sinking velocities of different size coccoliths were calculated by the cubic shape parameter 'b' as described in discussion part. We modeled the coccoliths sinking process and computed the separation ratio (Figure D1-b), coccolith length (Figure D1-c) and instant sinking velocities (Figure D1-d) at different time sections.

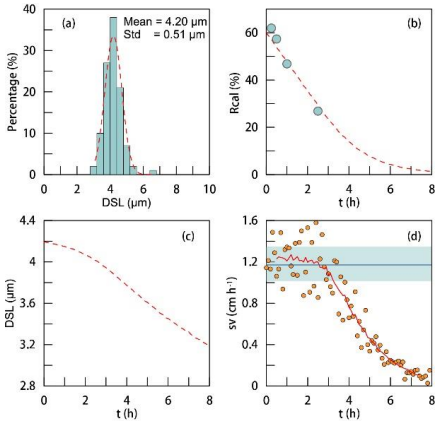

Biogeosciences Discuss., https://doi.org/10.5194/bg-2018-82
Manuscript under review for journal Biogeosciences
Discussion started: 27 February 2018

497 **Figure D1**. The simulations of coccoliths settling with different lengths: (a) the length distribution of
498 coccoliths. The green bars represent measured data and red dash line represents the best fit for normal
499 distribution. (b) The calibrated separation ratio: the green dots are measured data in our settling
500 experiments and the red dash line represents results obtained from Monte Carlo simulations. (c) The
501 average length of removed coccolith in simulations; (d) the sinking velocities of coccoliths: the orange
502 dots are instant sinking velocity calculated from derivation of Rcal, the red dash line is weighted
503 average for the instant sinking velocity. Blue line represents the average sinking velocity we measured
504 and the green shade area represents 95% confidence level of the measured velocity.

505 For *G. oceanica* experiments, the instant sinking velocity would not change significantly until
506 settling for more 3 hours. That means for all Rcal larger than 15% are safe for liner regressions. The
507 minimum safe number of Rcal will descend with the drop of dispersion degree of coccolith length
508 distribution. Hence our assumption for average sinking velocity and the use of liner regression are
509 proved to be reasonable.

Biogeosciences Discuss., https://doi.org/10.5194/bg-2018-82
Manuscript under review for journal Biogeosciences
Discussion started: 27 February 2018

Appendix E. Statistical and error analyses

The errors of measured separation ratio (R) and calculated sinking velocity (sv) are mainly caused by counting coccolith, the error of which fellows the Poisson distribution. To detect the influence of counting number on the result error, the error of separation ratio was simulated by 5000 times Monte Carlo calculations with assumptions that 'V1:V2=15:10' and 'n1=n2' (Figure E1). The result shows that the number of coccolith counted in the upper column draws more influence on the relative error ($|R-R_{95CL}|/R$). That means more coccolith in the upper suspension should be counted to make results more accurate. The slope of R-T was calculated by liner fitting with the intercept fixed on V1/(V1+V2). The error of sinking velocity was also calculated by 5000 times Monte Carlo simulations in the software Matlab.

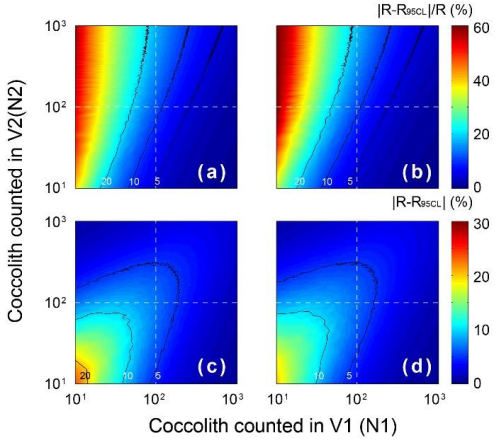

Figure E1. The error distribution with different N1 and N2 (ranging from 1 to 1000) simulated 5000 times by the Matlab with assumptions that the error distributions of N1 and N2 fellow Poisson distribution. The calculation of R follows equation 2-5, and here we assume numbers of FOV are equal (n1=n2). Counter lines mark values equal to 5, 10 and 20. (a) and (c) represent the lower 95% confidence level and (b) and (d) represent upper 95% confidence level. (a) and (b) the relative error of R and (c) and (d) represent the absolute error of R.